Ultra-deep sequencing reveals no evidence of oncogenic mutations or enrichment by *ex vivo* CRISPR/Cas9 genome editing in human hematopoietic stem and progenitor cells

M. Kyle Cromer[1]*, Valentin V. Barsan[1]*, Erich Jaeger[2], Mengchi Wang[2], Jessica P. Hampton[1], Feng Chen[2], Drew Kennedy[2], Irina Khrebtukova[2], Ana Granat[2], Tiffany Truong[2], Matthew H. Porteus[1]

[1]Department of Pediatrics, Stanford University, Stanford, CA 94305, USA

[2]Illumina, San Diego, CA USA

* These authors contributed equally to this work

† To whom correspondence should be addressed: mporteus@stanford.edu

Abstract

As CRISPR-based therapies enter the clinic, evaluation of the safety remains a critical and still active area of study. While whole genome sequencing is an unbiased method for identifying somatic mutations introduced by ex vivo culture and genome editing, this methodology is unable to attain sufficient read depth to detect extremely low frequency events that could result in clonal expansion. As a solution, we utilized an exon capture panel to facilitate ultra-deep sequencing of >500 tumor suppressors and oncogenes most frequently altered in human cancer. We used this panel to investigate whether transient delivery of high-fidelity Cas9 protein targeted to three different loci (using guide RNAs (gRNAs) corresponding to sites at AAVS1, *HBB*, and *ZFPM2*) at day 4 and day 10 timepoints post-editing resulted in the introduction or enrichment of oncogenic mutations. In three separate primary human HSPC donors, we identified a mean of 1,488 variants per Cas9 treatment (at <0.07% limit of detection). After filtering to remove germline and/or synonymous changes, a mean of 3.3 variants remained per condition, which were further reduced to six total mutations after removing variants in unedited treatments. Of these, four variants resided at the predicted off-target site in the myelodysplasia-associated *EZH2* gene that were subject to *ZFPM2* gRNA targeting in Donors 2 and 3 at day 4 and day 10 timepoints. While Donor 1 displayed on-target cleavage at *ZFPM2*, we found no off-target activity at *EZH2*. Sanger sequencing revealed a homozygous single nucleotide polymorphism (SNP) at position 14bp distal from the Cas9 protospacer adjacent motif in *EZH2* that eliminated any detectable off-target activity. We found no evidence of exonic off-target INDELs with either of the AAVS1 or HBB gRNAs. These findings indicate that clinically relevant delivery of high-fidelity Cas9 to primary HSPCs and *ex vivo* culture up to 10 days does not introduce or enrich for tumorigenic variants and that even a single SNP outside the seed region of the gRNA protospacer is sufficient to eliminate Cas9 off-target activity with this method of delivery into primary, repair competent human HSPCs.

Main

The CRISPR system, consisting of a CRISPR/Cas protein coupled with a guide RNA (gRNA), has demonstrated remarkable versatility for site-specific genome editing. To ensure safe clinical translation of CRISPR systems for genome editing, insertions and deletions (indels) should occur only at the intended genomic site without off-target effects, through either non-homologous end joining (NHEJ) or homology-directed repair (HDR) pathways. Unintended genome editing occurs through low-fidelity Cas enzymes or when the gRNA directs cleavage to sequences similar to the target sequence, leading to the incorporation of off-target mutations that may have oncogenic or otherwise deleterious consequences.

Several recent reports have shown that DNA double-strand breaks (DSBs) introduced by Cas9 initiate a p53 response in pluripotent and cancer cell lines that results in cell cycle arrest and/or apoptosis[1,2]. Because cells with loss-of-function mutations in p53 do not suffer the same degree of toxicity following genome editing and may proceed through the cell cycle with unresolved DSBs, these studies suggested that Cas9-mediated cleavage can enrich for p53 mutations. However, the findings from these studies depended on: 1) the presence of p53 mutations in the initial pool of cells prior to (not as a consequence of) Cas9 delivery, which would not be expected to occur in primary cells derived from healthy donors; 2) stably integrated Cas9 expressed by a strong, constitutive promoter, which reliably invoke a dramatic DNA damage response[3]; and 3) immortalized cell lines that typically have gross chromosomal abnormalities (polyploidy, aneuploidy, translocations, etc.) with dysfunctional DNA damage and nucleic acid delivery-sensing responses[4-6].

Significant efforts have thus been directed at not only predicting possible off-target genomic coordinates a priori[7-9], but also at the development of empirical wet lab-based methods for identifying sites of off-target activity following genome editing[10-14]. While these experimental methods reported activity at many candidate sites, which may be missed by *in silico* prediction methods, there is some concern that these techniques depart from Cas9 delivery in a clinical setting since these methods typically involve long-term constitutive expression of wild-type Cas9 in immortalized cell lines or cell-free genomic DNA (gDNA). Therefore, there is an urgent need to assess the performance of these prediction algorithms and empirical methods in more therapeutically relevant contexts (i.e., via transient ribonucleoprotein (RNP)-based delivery of high-fidelity Cas9[15] to human primary cells *ex vivo*).

The importance of long-term safety of genome editing/gene therapy in the clinic was illustrated recently when two sickle cell disease gene therapy trials (NCT02140554 and NCT04293185) were paused after two patients developed myeloid malignancies from either cytotoxic conditioning chemotherapy or insertional mutagenesis of the lentiviral vector[16]. Because of these safety concerns, in this study we sought to determine if oncogenic variants are introduced during Cas9 editing and/or the *ex vivo* expansion workflow. The ideal methodology necessitates targeted deep sequencing, however mutations with a variant allele frequency (VAF) below 1% remain mostly undetected by current genome-wide off-target detection techniques. This is in part because the signature of Cas9 nuclease activity is a spectrum of indels rather than primarily single nucleotide variants (SNVs). Therefore, an ultra-deep sequencing workflow capable of detecting SNVs as well as indels, amplifications, and multi-nucleotide variants (MNVs) has the potential to dramatically increase sensitivity for detection of the full spectrum of oncogenic off-target

editing activity from 1% to <0.1% VAF, which will be necessary to identify low frequency variants that could promote pathogenic clonal expansion.

Results

Novel sequencing pipeline attains high coverage of tumor suppressors and oncogenes

To perform ultra-deep sequencing of tumor suppressors and oncogenes, we used a hybrid-capture next-generation sequencing (NGS) assay for detection of DNA variants at high depth across the exons of 523 cancer-relevant genes (spanning 1.94 Mb) using unique molecular indexes (UMIs) (named TruSight Oncology 500 (TSO500))[17]. These genes comprise known oncogenes in key guidelines of the most common cancer types, spanning non-small cell lung cancer to pancreatic adenocarcinoma (Supplemental Table 1). Prior work has shown a high degree of concordance (both positive and negative agreement) between the TSO500 panel and whole exome sequencing for measurement of mutation burden (nonsynonymous mutations per kilobase of DNA)[17].

Hematopoietic stem and progenitor cells (HSPCs) from three separate healthy donors were subject to four conditions: Mock electroporated as well as three different Cas9 treatments with gRNAs targeting sites at AAVS1, *HBB*, or *ZFPM2* (Fig. 1A; Supplemental Table 2). Cas9 activity at AAVS1 and *HBB* have been thoroughly documented in the literature and these sites were chosen due to their relatively high and low off-target activity, respectively[11,12], and the *HBB* gRNA is currently in phase I clinical trials for correction of the single SNP responsible for sickle cell disease[18,19]. As a positive control that we expected to elicit off-target activity in the TSO500 panel, we designed a gRNA targeting intron 3 of *ZFPM2*, which has a predicted off-target site in exon 5 of *EZH2*. This off-target site differs by a single nucleotide at position 1 of the protospacer, the site furthest from the PAM, which has the least bearing on Cas9 specificity (Fig. 1B), and is the highest ranked off-target site for the *ZFPM2* guide by COSMID[7]. *EZH2* was chosen as a relevant positive control because of its well-characterized role in a wide range of tumor types[20,21] and the role of both loss- and gain-of-function mutations in myelodysplasias[22-25], making it especially relevant for HSPC editing.

The TSO500 genome editing workflow was adapted from a formalin-fixed paraffin-embedded (FFPE) tissue workflow to gDNA harvested from primary $CD34^+$-purified umbilical cord blood-derived HSPCs from three separate healthy donors. Frozen cells were thawed and expanded for 2 days in HSPC media at 100K cells/mL and then targeted in the four treatment groups (2-5x10^5 cells per treatment group) as reported previously[18,19,26,27] (Fig. 1A). Genomic DNA was then harvested from 3-4x10^5 cells at day 0 to establish germline variants and then cells were split into treatment groups, electroporated, and re-plated in fresh media. Because prior reports have shown that indel formation reaches completion 4 days after electroporating HSPCs with Cas9 RNP[27], we harvested 4x10^5 cells from each treatment group at day 4 and extracted gDNA for analysis. To determine whether enrichment of tumorigenic variants was occurring in our *ex vivo*-expanded HSPC populations, as well as to gain insight into whether *ex vivo* expansion itself (independent of Cas9 activity) was enriching for tumorigenic variants, we also harvested gDNA from the remainder of cells at 10 days post-targeting.

To ensure that high levels of on-target activity occurred for each gRNA, we performed targeted PCR amplification of the genomic region surrounding the predicted cut site followed by Sanger sequencing and

analysis of indels by TIDE[28]. Indeed, a high frequency of on-target indels were observed across all three donors for AAVS1 and *HBB* gRNAs (Fig. 1C). While consistent across all donors, the *ZFPM2* gRNA induced fewer indels, which is not surprising due to its high degree of predicted off-target activity as well as the fact that this guide was not screened for efficiency prior to inclusion in this study, in contrast to the AAVS1 and HBB gRNAs that were identified as high activity gRNAs after screening multiple guides.

Pilot experiments were performed to confirm that the pipeline may be adapted from FFPE-derived tissue to gDNA harvested from primary cells. To determine the optimal amount of DNA for application to the sequencing pipeline, a range of 10-30ng of DNA was used as input for library preparation using the hybrid capture-based TSO500 Library Preparation Kit. Reads were mapped to the human genome (build hg19) and raw sequencing data was processed through a custom bioinformatic pipeline (Supplemental Fig. 1A) to identify indels, SNVs, and MNVs. Pilot experiments confirmed successful adaptation of the sequencing pipeline to gDNA harvested from primary cells in culture, and that at least 30ng of input DNA was necessary to achieve a median exon coverage (MEC) of 2000 (Supplemental Fig. 1B). To simultaneously detect intended edits, we supplemented the TSO500 panel with probes specific to AAVS1, *HBB*, and *ZFPM2* (Supplemental Table 3).

Following initial pilot experiments, raw sequencing data yielded a mean MEC >3550 for all samples per technical replicate, corresponding to a minimum limit of detection (LoD) and sensitivity of 0.205% and 95%, respectively (Fig. 2A; Supplemental Fig. 2). Moreover, because three technical replicates were sequenced for almost all timepoints and conditions, which are factored into the mean MEC of >3550, our LoD in these samples was further pushed to a limit of <0.07% VAF. Variants were consistent across technical replicates in terms of the types of variants called, with no significant differences comparing Mock to Cas9 treatments (Fig. 2B). We also observed a high degree of concordance across technical replicates, with a median of 98.31% of variants called in all replicates for each treatment for each donor (Fig. 2C; Supplemental Table 4). These data indicated that the total number of variants across replicates was more dependent on donor of origin than either time in culture or treatment with Cas9. In addition, the number of variants within each donor did not consistently increase due to time in culture (i.e., day 0 v. day 4 v. day 10) or treatment with Cas9. Consistent with these results, we found that read depth across the genome was more heavily influenced by donor than any other factor (Supplemental Fig. 3). In addition, while chromothripsis was recently reported as a rare consequence of on-target Cas9 cleavage[29], in our bulk population of HSPCs we found no apparent drop in read depth in variants proximal to the intended cut site for any Cas9 treatment.

Few variants found in treatments after filtering non-pathogenic germline mutations

To gain insight into the characteristics of the variants identified in our cohort, we plotted VAF by MEC for Mock samples at days 0, 4, and 10 (Supplemental Fig. 4A). Strikingly for all donors across all timepoints, the VAF frequencies trend toward 0.5 and 1.0 as MEC increases, which would correspond to heterozygous and homozygous germline variants, respectively. Because all variants were found within a panel of tumor suppressors and oncogenes, yet all HSPCs were derived from normal, healthy donors, we expect virtually all variants identified in Day 0 and Mock conditions to be non-pathogenic. Indeed, when filtering out both synonymous variants as well as those previously reported to occur >10 times in comprehensive germline databases[30,31], an extremely small number of variants remain (a mean of 3.9 variants remaining from 1,490.1 reproducible variants per condition). Again, we found no consistent

increase in the number of variants as HSPCs were cultured from d0 to d10. Interestingly, we observed several consistent variants that, while present in our germline database and consequently filtered, were found at intermediate VAFs rather than trending toward 0.5 or 1.0. While these variants were extremely consistent within, but not across donors, none of these were found in the exons of genes associated with clonal hematopoiesis of indeterminate potential[32,33] (Note: the age of the donors for the source of the HSPCs is not known). Therefore, we believe these mutations represent either sequencing artefacts or bona fide HSPC donor chimerism that occurred prior to *ex vivo* culture or editing.

To determine whether editing with Cas9 introduces variants in tumor suppressors or oncogenes, we then plotted VAF x MEC for all Cas9 treatment groups at days 4 and 10 for all three donors (Fig. 2D; Supplemental Fig. 4B). Again, as expected for heterozygous and homozygous germline mutations, unfiltered variants trend toward VAFs of 0.5 and 1.0 as MEC increases. We next filtered out non-pathogenic variants by eliminating all called mutations that are synonymous and/or have been previously reported in the germline variant database. We found that our Cas9 treatments had a fewer number of variants remaining than even our Mock conditions (a mean of 3.3 variants remaining from 1,487.9 reproducible variants per condition). Because any variants also found in our Mock samples would not have been introduced by Cas9, we then removed all variants present in Mock conditions within each donor and only six variants remain among all eighteen Cas9 treatments (Fig. 3A). Of the six remaining variants, four of these are the expected *EZH2* mutations in Donors 2 and 3 within both day 4 and day 10 *ZFPM2* treatments. The other two variants that remain after filtering germline, synonymous, and Mock mutations are both SNVs found in d10 *ZFPM2* treatments in Donors 2 and 3 at <0.0015 VAF, which is close to our limit of detection. It is important to note that while only six variants remained in our treatment groups, the filters we applied to our Cas9 conditions were extremely conservative. Because Cas9 introduces indels far more frequently than SNVs at sites that display homology to the gRNA, if we apply these additional filters to our variants (i.e., remove SNVs as well as sites with no homology to the gRNA), only *EZH2* mutations remain.

EZH2 off-target activity eliminated by homozygous SNP in Cas9 gRNA protospacer

In Donors 2 and 3, the expected *EZH2* off-target site displayed the highest VAF in both day 4 and day 10 timepoints across all three replicates at high confidence (3,893x average coverage) at an average of 19.3% off-target activity (Fig. 3A). Interestingly, the *EZH2* VAF in these donors decreased from day 4 to day 10 (mean of 21.7% to 16.9%, respectively), indicating a possible selective disadvantage for cells that harbor indels in this gene. The indel spectrum within *EZH2* was characterized (Supplemental Fig. 5) and total frequency was validated by PCR amplification, Sanger sequencing, and analysis of indels by TIDE (Fig. 3B). Notably, even without filtering Mock variants, mutations in *EZH2* comprised the vast majority of calls in Cas9 treatments in Donors 2 and 3 (Fig. 3C; Supplemental Fig. 6). Surprisingly, we found no detectable off-target activity at *EZH2* in Donor 1 by either NGS or TIDE (Fig. 3B) despite a high degree of on-target activity at *ZFPM2*. Upon investigation of the Sanger trace at this site in Donor 1, we found a homozygous SNP at position 6 of the protospacer. Due to the specificity of high-fidelity Cas9, which has been reported to reliably reduce off-target activity by 20-fold[15], it is likely that this homozygous SNP eliminated all activity at this site (below the detection threshold of the TSO500 panel). The exceptional specificity of high-fidelity Cas9, when transiently delivered to primary cells, is evident from the single SNP outside of the core region of the protospacer in Donor 1 that was sufficient to eliminate all detectable activity at this site.

Whole exome sequencing confirms absence of off-target activity from ex vivo culture & genome editing

Because transient delivery of Cas9 RNP and up to 10 days of ex vivo culture elicited few variants in the TSO500 panel, we next sought to expand our search for off-target activity to the entire exome. To do so, we electroporated high-fidelity Cas9 pre-complexed with AAVS1 gRNA to a single HSPC donor. We used the AAVS1 gRNA because it has been described as less specific than the HBB gRNA and we wanted to increase the chances of detecting any exonic off-target site. We then harvested gDNA from AAVS1-targeted and Mock electroporated treatments at d10 post-editing and subjected these to an exome capture panel and NGS. Prior to filtering, we identified 38,431 and 38,527 variants in Mock and AAVS1 treatments, respectively (Fig. 4A). To identify variants that may have resulted from Cas9 treatment, a tumor-normal pipeline was used to call somatic variants that were unique to the AAVS1 treatment ("tumor") after subtracting the Mock as background ("normal"). In addition, we inverted the tumor-normal designation (i.e., treating Mock as tumor and AAVS1 treatment as normal) in order to estimate our background frequency of somatic calls resulting from this pipeline. These analyses identified 137 somatic variants in the AAVS1 treatment and 92 variants in the Mock condition (Fig. 4B). Because this pipeline is typically used to identify somatic variants in heterogeneous tumor samples, any mutation with a VAF notably greater than the "normal" sample was flagged. However, no off-target mutation introduced by Cas9 would have been present at any detectable VAF in the Mock condition. Therefore, we removed any variants found at >0.01 VAF in the Mock treatment, leaving 30 somatic mutations for further analysis (Fig. 4C). Though Cas9 nuclease activity typically introduces indels surrounding sites with a high degree of homology to the protospacer sequence, the majority of remaining variants after filtering (17/30) were SNVs and none of the 30 mutations were found to have >10bp match to the protospacer + PAM sequence within 20bp upstream or downstream of the called variant. We therefore conclude that neither targeted tumor suppressor/oncogene sequencing nor WES was able to identify any somatic mutations that occurred as a consequence of Cas9 activity. We therefore believe that the variants identified as somatic mutations in both Mock and AAVS1 treatments represent either real variation that occurred over the course of the 10 day ex vivo HSPC expansion or are sequencing artefacts.

Discussion

The first CRISPR-based therapies have entered early human clinical trials and many others are entering drug development pipelines[34]. There is a growing need to establish the long-term safety of edited human cells (*ex vivo* and *in vivo*) by CRISPR nucleases and vectors. Establishing the appropriate metrics for assessing genomic stability after genome editing continues to be an important and active area of study. For instance, whereas WGS is the only way to capture variants/abnormalities across the entire genome, read depth per base pair to achieve high sensitivity needed for genome editing purposes across a population of cells is not technically feasible. Sequencing the entire human genome only allows detection of high frequency events due to low per-base coverage. Alternatively, limiting sequencing to the most conserved and frequently mutated regions of the genome (e.g., exons, which comprises 1% of the genome[35]) allows for greater coverage and therefore greater detection power of lower frequency variants. Because cancer can occur due to expansion of even a single mutated clone, in this study we applied this

concept to further limit sequencing to exons of the most common tumor suppressors and oncogenes to detect extremely low frequency events.

Cas9 is able to initiate DSBs in the DNA at both on- and off-target sites, potentially leading to unintended genomic abnormalities. In fact, several studies reported the enrichment of p53-inactivating mutations following CRISPR-based editing in immortalized human cell lines with constitutive or inducibly expressed Cas9 when a subset of p53 mutant cells were spiked in[1,2]. In contrast, prior studies in human primary cells found that Cas9 RNP delivery did not introduce mutations in p53 or 129 other cancer-related genes (using the Stanford Solid Tumor Actionable Mutation Panel)[36,37]. Therefore, we developed a novel tumor suppressor/oncogene ultra-deep sequencing pipeline to determine whether editing and short-term *ex vivo* expansion leads to disruption and/or enrichment of cancer-associated variants when delivered in a clinically relevant context—i.e., when high-fidelity Cas9[15] is transiently delivered as RNP via electroporation to human primary HSPCs without subpopulations of cells with pre-existing tumorigenic variants. Toward this end, our workflow interrogated the exons of 523 known tumor suppressors and oncogenes and achieved levels of detection of germline and somatic mutations at <0.1% VAF.

When editing with three separate gRNAs (targeting AAVS1, *HBB*, and *ZFPM2*), with ultra-deep sequencing of >500 tumor suppressors and oncogenes found no detectable variants (>0.002 VAF) that could be attributed to Cas9 activity or *ex vivo* expansion (aside from the expected *EZH2* off-target site in the *ZFPM2* treatment group). These findings were further confirmed by the absence of any off-target activity at sites resembling the AAVS1 gRNA by WES. In this clinically relevant context, transiently delivered high-fidelity Cas9 RNP into primary HSPCs did not introduce or enrich tumor variants. In fact, high-fidelity Cas9 was found to be so specific that even a single homozygous SNP at position 6 of the protospacer eliminated all detectable off-target activity in *EZH2*. In light of our findings, previous reports[1,2] are likely an artefact of p53 mutant spike-in, genomic instability of cell lines, supraphysiological levels of Cas9 expression, and/or dramatic toxicity. Taken together, this work highlights the importance of: 1) regulating the duration and level of nuclease expression in order to limit the degree of off-target activity[12,38]; 2) minimizing toxicity through electroporation of RNP as opposed to mRNA- or plasmid-based editing[39] so that opportunities for clonal expansion are minimized; and 3) conducting experiments in the most clinically relevant models—primary human cells with functional DNA sensing and damage repair machinery—rather than immortalized cell lines with well documented genomic abnormalities[4,5].

A limitation of this work is that we focused entirely on the coding regions of genes, including those known to be involved in cancer. We chose this focus as off-target effects in coding regions, especially in tumor suppressor genes, might carry the highest risk for causing a serious adverse event. This focus, however, enabled high sequencing depth. Nonetheless, off-target INDELs in the non-coding region of the genome were not evaluated.

The importance of establishing safety of cell-based therapies prior to clinical translation is illustrated by the recent development of leukemia in two patients enrolled in a lentiviral gene therapy trial for sickle cell disease, which resulted in pausing of both related trials[16]. Follow-up investigation found that leukemic cells harbor viral integrations and that mutations in *RUNX1* and *PTPN11* occurred at some point during or following myeloablative conditioning and/or lentiviral integration. Disruption of both of genes have been shown to play a role in a wide variety of cancers[40-43], and due to inclusion in the TSO500 panel and the sequencing depth we achieved in this study, we would have been able to identify variants in these genes at $\geq$0.1% VAF prior to autologous transplantation in these trials. Therefore, we believe that

our study not only establishes an important benchmark for the typical degree of variation in cancer-associated genes following CRISPR-based editing and short-term *ex vivo* expansion, but also may become a common tool for assessing safety of cell-based products prior to transplantation (particularly in the event of clonal expansion and/or long-term *ex vivo* expansion). In doing so, we hope to maximize the long-term safety of the new generation of site-specific genome editing therapies. As CRISPR/Cas9 editing becomes more clinically widespread, identification and avoidance of genotoxicity will profoundly impact the pace with which these curative approaches reach patients safely.

Acknowledgements

V.B. is an Anne T. and Robert M. Bass Endowed Fellow, supported by the Stanford Child Health Research Institute.

Author Disclosures

The authors of this study also wish to declare the following conflicts of interest: M.H.P. is a member of the scientific advisory board of Allogene Therapeutics. M.H.P. is on the Board of Directors of Graphite Bio. M.H.P. serves on the SAB of Allogene Tx and is an advisor to Versant Ventures. M.H.P. and M.K.C. have equity in Graphite Bio. M.H.P. has equity in CRISPR Tx. E.J., M.W., F.C., D. K., and J. X. are employees of Illumina, Inc.

Methods

Culturing of HSPCs

Primary human HSPCs were sourced from fresh umbilical cord blood (generously provided by Binns Family program for Cord Blood Research) under protocol 33818, which was approved and renewed annually by the NHLBI IRB. All patients provided informed consent for the study. $CD34^+$ HSPCs were bead-enriched using Human CD34 Microbead Kits (Mitenyi Biotec, Inc., Bergisch Gladbach, Germany) according to manufacturer's protocol and cultured at 1×10^5 cells/mL in CellGenix GMP SCGM serum-free base media (Sartorius CellGenix GmbH, Freiburg, Germany) supplemented with stem cell factor (SCF)(100ng/mL), thrombopoietin (TPO)(100ng/mL), FLT3–ligand (100ng/mL), IL-6 (100ng/mL), UM171 (35nM), 20mg/mL streptomycin, and 20U/mL penicillin. The cell incubator conditions were 37°C, 5% CO_2, and 5% O_2.

Genome editing of HSPCs

Chemically modified sgRNAs used to edit HSPCs were purchased from Synthego (Menlo Park, CA, USA). The sgRNA modifications added were the 2'-O-methyl-3'-phosphorothioate at the three terminal nucleotides of the 5' and 3' ends described previously[38]. All Cas9 protein (SpyFi S.p. Cas9 nuclease) was purchased from Aldevron, LLC (Fargo, North Dakota, USA). The RNPs were complexed at a Cas9:sgRNA molar ratio of 1:2.5 at 25°C for 10min prior to electroporation. HSPCs were resuspended in P3 buffer (Lonza, Basel, Switzerland) with complexed RNPs and electroporated using the Lonza 4D Nucleofector (program DZ-100). Cells were plated at $1x10^5$ cells/mL following electroporation in the cytokine-supplemented media described above.

TSO500 library preparation

Input DNA concentration was determined by Qubit dsDNA HS assay kit on the Qubit Fluorometer according to the manufacturing protocol (Qubit, London, UK). DNA was then fragmented to 90 to 250 bp by sonication using a Covaris E220 Evolution Sonicator (Covaris, Woburn, MA, USA), with a target peak of around 130bp as determined by Agilent Technologies 2100 Bioanalyzer using a High Sensitivity DNA chip. Samples then underwent end repair and A-tailing. Adapters containing UMIs were ligated to the ends of the DNA fragments. After a purification step, the DNA fragments were amplified using primers to add index sequences for sample multiplexing (required for cluster generation). Two hybridization/capture steps were performed. First, a pool of oligos specific to the 523 genes targeted by TSO500 with supplementary probes from IDT (Supplementary Table 3) were hybridized to the prepared DNA libraries overnight. Next, streptavidin magnetic beads were used to capture probes hybridized to the targeted regions. The hybridization and capture steps were repeated using the enriched DNA libraries to ensure high specificity for the captured regions. Primers were used to amplify the enriched libraries using sample purification beads. The enriched libraries were quantified and each library was normalized to ensure a uniform representation in the pooled libraries. Finally, the libraries were pooled, denatured, and diluted to the appropriate loading concentration and sequenced on an Illumina NovaSeq with a read length of 2x151 base pairs. Up to 8 TSO500 libraries were sequenced per run.

Indel frequency analysis by TIDE

2-4d post-targeting, HSPCs were harvested and a Qiagen DNeasy Blood & Tissue Kit (Redwood City, CA, USA) was used to collect gDNA. The following primers were then used to amplify respective cut sites at with Phusion Green Hot Start II High-Fidelity PCR Master Mix (Thermo Fisher Scientific, Waltham, MA, USA) according to manufacturer's instructions: AAVS1, forward: 5'-AGGATCCTCTCTGGCTCCAT-3', reverse: 5'-CCCCTGTCATGGCATCTTC-3'; *HBB*, forward: 5'-AGGGTTGGCCAATCTACTCC-3', reverse: 5'-AGTCAGTGCCTATCAGAAACCCAAGAG-3'; *ZFPM2*, forward: 5'-GCAAATGCAGCAGTAGACCA-3', reverse: 5'-CCTTCGCTCTCAATTTTGCT-3'; and *EZH2* (*ZFPM2* OT1), forward: 5'-AAAAGAGAAAGAAGAAACTAAGCCCTA-3', reverse: 5'-TTTTCCTCCCCTCATTTCAA-3'. PCR reactions were then run on a 1% agarose gel and appropriate bands were cut and gel-extracted using a GeneJET Gel Extraction Kit (Thermo Fisher Scientific, Waltham, MA, USA) according to manufacturer's instructions. Gel-extracted amplicons were then Sanger sequenced with the forward and reverse amplicon primers shown above. Resulting Sanger chromatograms were then used as input for indel frequency analysis by TIDE as previously described[26].

Whole-exome sequencing

Data was processed using the DRAGEN v3.8.4 Enrichment pipeline. All datasets were processed as independent samples, and related mock and test samples were additionally processed as "tumor/normal" and "normal/tumor" pairs. Known systematic noise filters were applied to all called variants.

References

1. Ihry, R.J. et al. p53 inhibits CRISPR-Cas9 engineering in human pluripotent stem cells. *Nat Med* **24**, 939-946 (2018).
2. Haapaniemi, E., Botla, S., Persson, J., Schmierer, B. & Taipale, J. CRISPR-Cas9 genome editing induces a p53-mediated DNA damage response. *Nat Med* **24**, 927-930 (2018).
3. Morgens, D.W. et al. Genome-scale measurement of off-target activity using Cas9 toxicity in high-throughput screens. *Nat Commun* **8**, 15178 (2017).
4. Passerini, V. et al. The presence of extra chromosomes leads to genomic instability. *Nat Commun* **7**, 10754 (2016).
5. Yoshihara, M., Oguchi, A. & Murakawa, Y. Genomic Instability of iPSCs and Challenges in Their Clinical Applications. *Adv Exp Med Biol* **1201**, 23-47 (2019).
6. Mittelman, D. & Wilson, J.H. The fractured genome of HeLa cells. *Genome Biol* **14**, 111 (2013).
7. Cradick, T.J., Qiu, P., Lee, C.M., Fine, E.J. & Bao, G. COSMID: A Web-based Tool for Identifying and Validating CRISPR/Cas Off-target Sites. *Mol Ther Nucleic Acids* **3**, e214 (2014).
8. Stemmer, M., Thumberger, T., Del Sol Keyer, M., Wittbrodt, J. & Mateo, J.L. CCTop: An Intuitive, Flexible and Reliable CRISPR/Cas9 Target Prediction Tool. *PLoS One* **10**, e0124633 (2015).
9. Bae, S., Park, J. & Kim, J.S. Cas-OFFinder: a fast and versatile algorithm that searches for potential off-target sites of Cas9 RNA-guided endonucleases. *Bioinformatics* **30**, 1473-5 (2014).
10. Tsai, S.Q. et al. GUIDE-seq enables genome-wide profiling of off-target cleavage by CRISPR-Cas nucleases. *Nat Biotechnol* **33**, 187-197 (2015).
11. Tsai, S.Q. et al. CIRCLE-seq: a highly sensitive in vitro screen for genome-wide CRISPR-Cas9 nuclease off-targets. *Nat Methods* **14**, 607-614 (2017).
12. Cameron, P. et al. Mapping the genomic landscape of CRISPR-Cas9 cleavage. *Nat Methods* **14**, 600-606 (2017).
13. Lazzarotto, C.R. et al. CHANGE-seq reveals genetic and epigenetic effects on CRISPR-Cas9 genome-wide activity. *Nat Biotechnol* **38**, 1317-1327 (2020).
14. Wienert, B. et al. Unbiased detection of CRISPR off-targets in vivo using DISCOVER-Seq. *Science* **364**, 286-289 (2019).
15. Vakulskas, C.A. et al. A high-fidelity Cas9 mutant delivered as a ribonucleoprotein complex enables efficient gene editing in human hematopoietic stem and progenitor cells. *Nat Med* **24**, 1216-1224 (2018).
16. NHLBI. Statement on NHLBI decision to pause the Pilot and Feasibility Study of Hematopoietic Stem Cell Gene Transfer for Sickle Cell Disease. (2021).
17. Zhao, C.J., T.; Ju, J.H.; Zhang, S.; Tao, J.; Fu, Y.; Lococo, J.; Dockter, J.; Pawlowski, T; Bilke, S. TruSight Oncology 500: Enabling Comprehensive Genomic
Profiling and Biomarker Reporting with Targeted Sequencing. *bioRxiv* (2020).
18. Dever, D.P. et al. CRISPR/Cas9 beta-globin gene targeting in human haematopoietic stem cells. *Nature* **539**, 384-389 (2016).
19. Bak, R.O., Dever, D.P. & Porteus, M.H. CRISPR/Cas9 genome editing in human hematopoietic stem cells. *Nat Protoc* **13**, 358-376 (2018).
20. Kim, K.H. & Roberts, C.W. Targeting EZH2 in cancer. *Nat Med* **22**, 128-34 (2016).
21. Cromer, M.K. et al. Identification of somatic mutations in parathyroid tumors using whole-exome sequencing. *J Clin Endocrinol Metab* **97**, E1774-81 (2012).
22. Béguelin, W. et al. EZH2 is required for germinal center formation and somatic EZH2 mutations promote lymphoid transformation. *Cancer Cell* **23**, 677-92 (2013).
23. Morin, R.D. et al. Somatic mutations altering EZH2 (Tyr641) in follicular and diffuse large B-cell lymphomas of germinal-center origin. *Nat Genet* **42**, 181-5 (2010).

24. Göllner, S. et al. Loss of the histone methyltransferase EZH2 induces resistance to multiple drugs in acute myeloid leukemia. *Nat Med* **23**, 69-78 (2017).
25. Guglielmelli, P. et al. EZH2 mutational status predicts poor survival in myelofibrosis. *Blood* **118**, 5227-34 (2011).
26. Cromer, M.K. et al. Gene replacement of alpha-globin with beta-globin restores hemoglobin balance in beta-thalassemia-derived hematopoietic stem and progenitor cells. *Nat Med* **27**, 677-687 (2021).
27. Charlesworth, C.T. et al. Priming Human Repopulating Hematopoietic Stem and Progenitor Cells for Cas9/sgRNA Gene Targeting. *Mol Ther Nucleic Acids* **12**, 89-104 (2018).
28. Brinkman, E.K., Chen, T., Amendola, M. & van Steensel, B. Easy quantitative assessment of genome editing by sequence trace decomposition. *Nucleic Acids Res* **42**, e168 (2014).
29. Leibowitz, M.L. et al. Chromothripsis as an on-target consequence of CRISPR-Cas9 genome editing. *Nat Genet* **53**, 895-905 (2021).
30. Karczewski, K.J. et al. The mutational constraint spectrum quantified from variation in 141,456 humans. *Nature* **581**, 434-443 (2020).
31. Genomes Project, C. et al. A global reference for human genetic variation. *Nature* **526**, 68-74 (2015).
32. Heuser, M., Thol, F. & Ganser, A. Clonal Hematopoiesis of Indeterminate Potential. *Dtsch Arztebl Int* **113**, 317-22 (2016).
33. Feusier, J.E. et al. Large-Scale Identification of Clonal Hematopoiesis and Mutations Recurrent in Blood Cancers. *Blood Cancer Discov* **2**, 226-237 (2021).
34. Mullard, A. Gene-editing pipeline takes off. *Nat Rev Drug Discov* **19**, 367-372 (2020).
35. Choi, M. et al. Genetic diagnosis by whole exome capture and massively parallel DNA sequencing. *Proc Natl Acad Sci U S A* **106**, 19096-101 (2009).
36. Vaidyanathan, S. et al. Targeted replacement of full-length CFTR in human airway stem cells by CRISPR-Cas9 for pan-mutation correction in the endogenous locus. *Mol Ther* (2021).
37. Gomez-Ospina, N. et al. Human genome-edited hematopoietic stem cells phenotypically correct Mucopolysaccharidosis type I. *Nat Commun* **10**, 4045 (2019).
38. Hendel, A. et al. Chemically modified guide RNAs enhance CRISPR-Cas genome editing in human primary cells. *Nat Biotechnol* **33**, 985-989 (2015).
39. Cromer, M.K. et al. Global Transcriptional Response to CRISPR/Cas9-AAV6-Based Genome Editing in CD34. *Mol Ther* **26**, 2431-2442 (2018).
40. Sood, R., Kamikubo, Y. & Liu, P. Role of RUNX1 in hematological malignancies. *Blood* **129**, 2070-2082 (2017).
41. Chan, G., Kalaitzidis, D. & Neel, B.G. The tyrosine phosphatase Shp2 (PTPN11) in cancer. *Cancer Metastasis Rev* **27**, 179-92 (2008).
42. Mohi, M.G. & Neel, B.G. The role of Shp2 (PTPN11) in cancer. *Curr Opin Genet Dev* **17**, 23-30 (2007).
43. Janes, K.A. RUNX1 and its understudied role in breast cancer. *Cell Cycle* **10**, 3461-5 (2011).

Figure 1: Experimental design & confirmation of on-target activity.

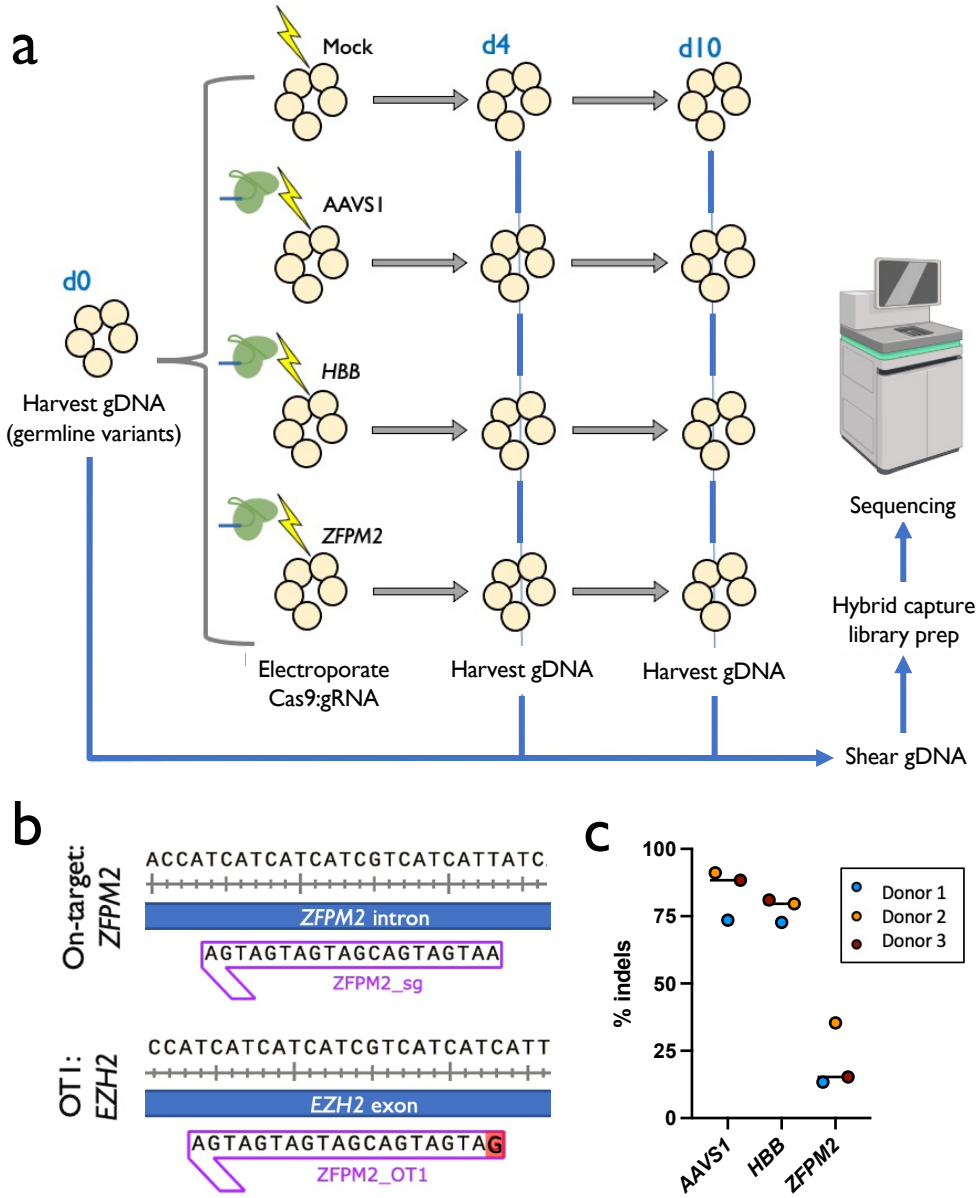

a) Experimental design: CD34^{+} HSPCs from 3 donors underwent gDNA harvesting at d0 (to establish germline variants) and were then subject to mock electroporation or Cas9 treatments with gRNAs corresponding to sites at AAVS1, *HBB*, and *ZFPM2*. Cells were cultured and gDNA was harvested again at d4 and 10.

b) Predicted off-target cut site (OT1) of *ZFPM2* guide in exon 5 of the *EZH2* gene, based on sequence homology. Mismatch in gRNA is shown in red.

c) On-target activity of AAVS1, *HBB*, and *ZFPM2* gRNAs determined by PCR amplification of the genomic region surrounding the predicted cut sites followed by Sanger sequencing and analysis of indels by TIDE 4 days post-targeting. Bars represent median. N=3 separate HSPC donors.

Figure 2: Summary of sequencing data.

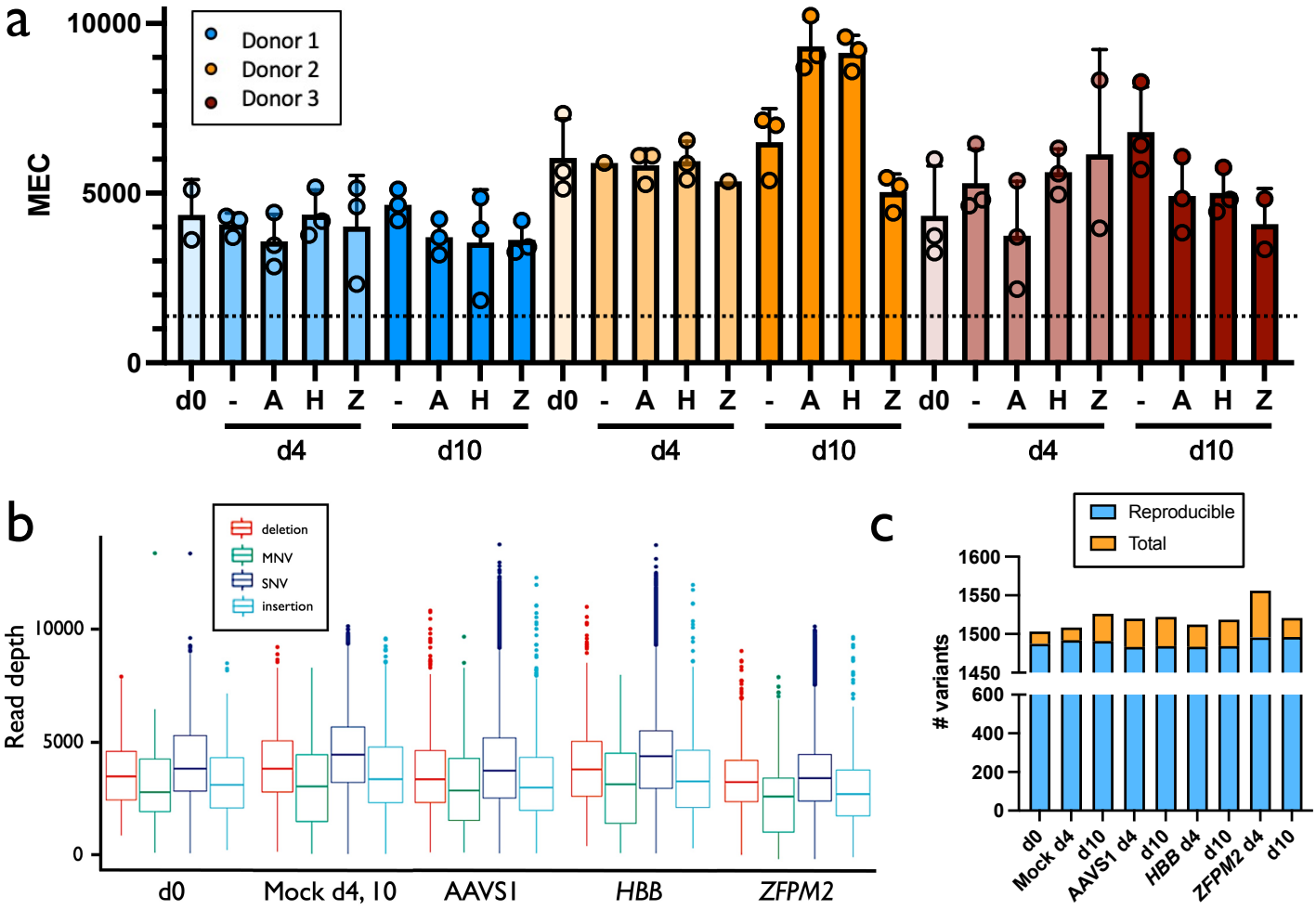

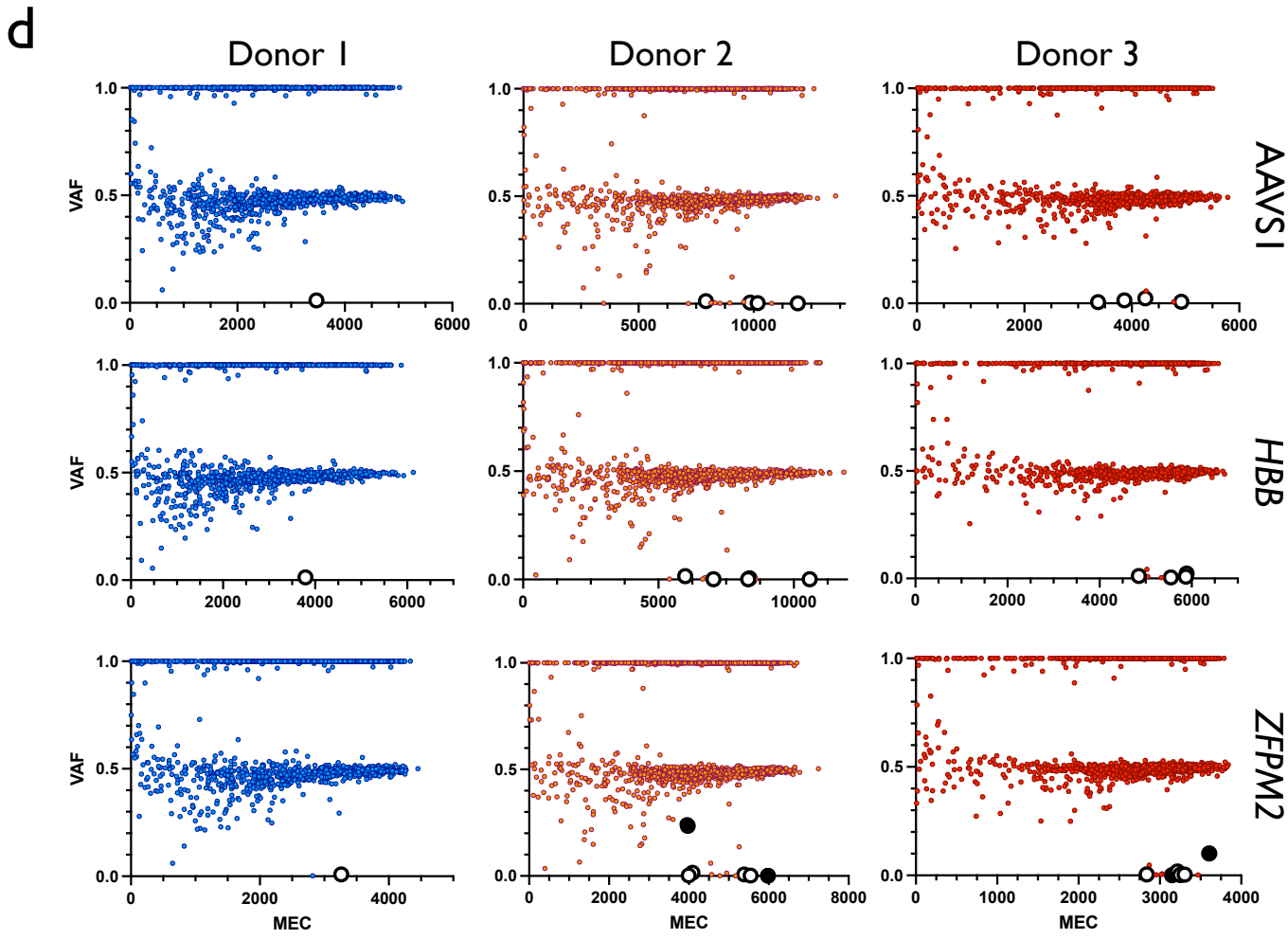

a) MEC for each treatment for each donor. Treatments are Mock electroporated (-), AAVS1- (A), *HBB*- (H), and *ZFPM2*-targeted (Z). Individual points represent technical replicates. Columns and error bars represent mean and standard deviation.

b) MEC across all timepoints for each condition demonstrates consistent deep coverage for indels, SNVs, and MNVs. Midline represents median and box represents 25th through 75th percentiles. Variants among all donors and timepoints are combined for Cas9 treatments. In d0 and Mock, all donors are combined.

c) Number of reproducible variants across technical replicates from total called by treatment group. Columns represent mean variants called for the three donors within each treatment.

d) VAF x MEC for all variants found among technical replicates for Cas9 treatments for each donor at d10. Large white points are those that remained after removing germline and synonymous variants. Large black points are those that remain after removing variants present in Mock within each donor.

Figure 3:Variants identified in Cas9 treatments.

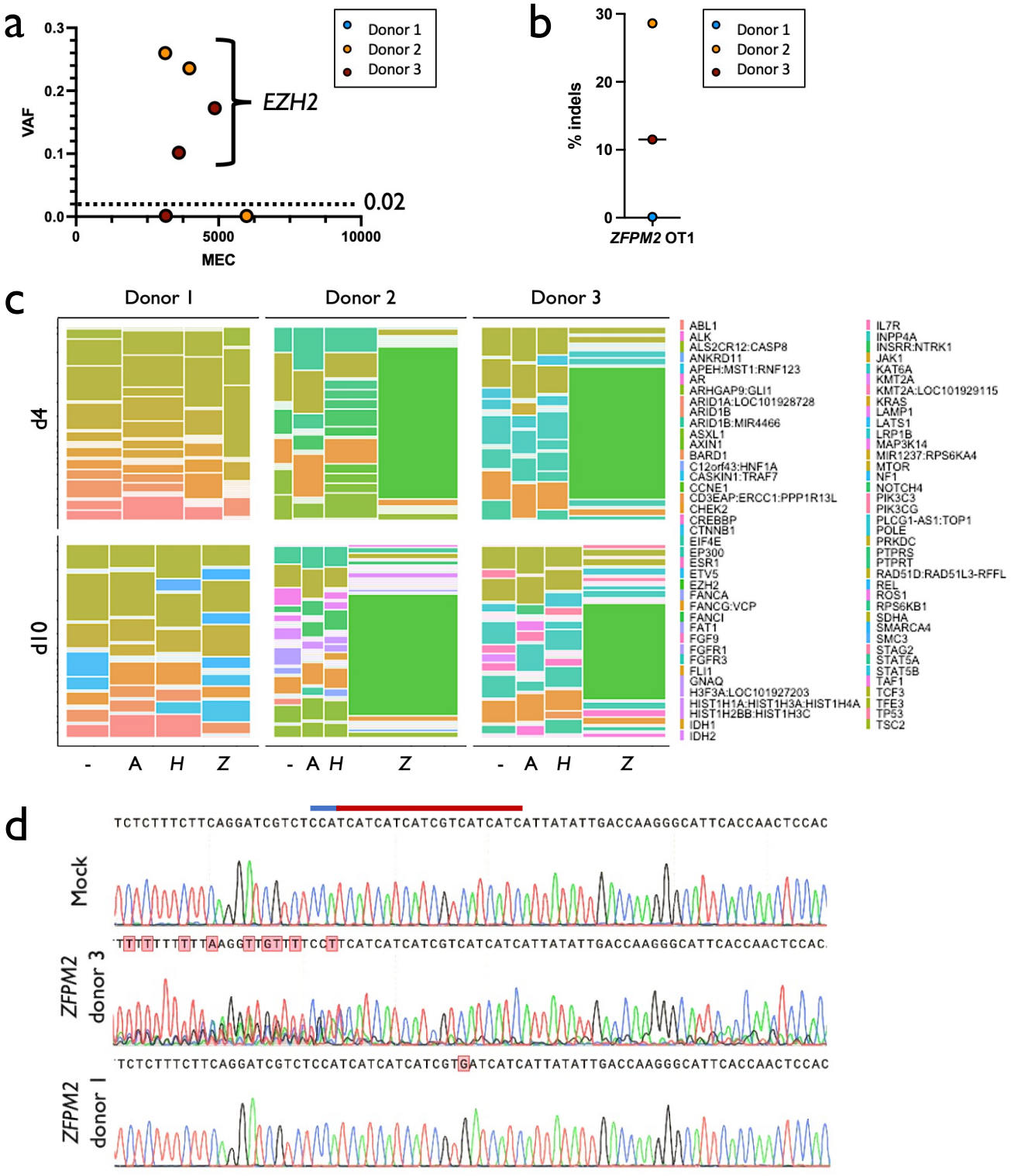

a) VAF x MEC for variants remaining from all Cas9 treatments after removal of synonymous, germline, and Mock calls. Donor 1 had no variants remaining after filtering.

b) Percent indels in *EZH2* identified by PCR amplification, Sanger sequencing, and TIDE analysis in d4 gDNA. Donor 1 had no detectable activity.

c) Mosaic plot of genes harboring mutations within each donor and Cas9 treatment at d4 and 10. Area is proportional to the number of times variants were called in a particular gene within a particular treatment group. Filtering removed germline and synonymous variants. For each donor and timepoint, conditions are ordered as mock, AAVS1, *HBB*, and *ZFPM2* (-, A, *H*, and *Z*, respectively).

d) Sanger chromatograms at predicted *EZH2* off-target site. The PAM site and protospacer are depicted as blue and red lines, respectively. Homozygous SNP in Donor 1 abrogated detectable editing activity.

Figure 4:Variants identified in whole exome sequencing.

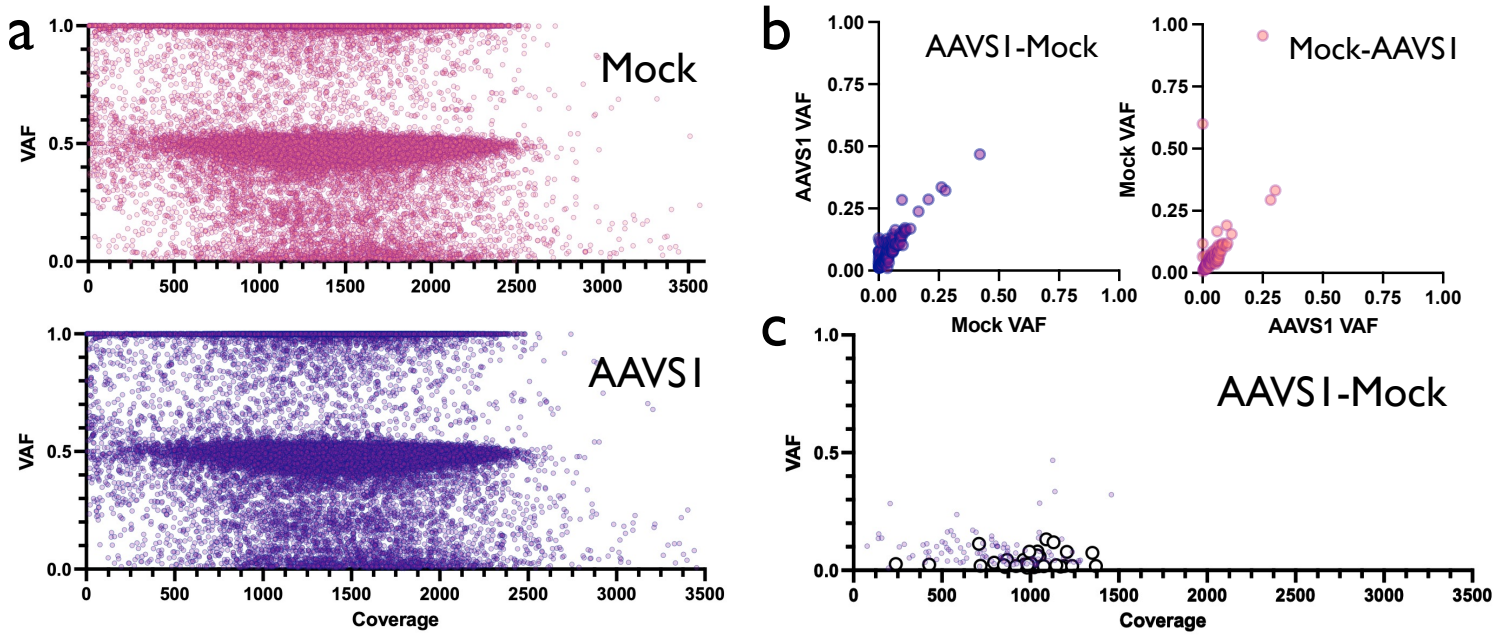

d

Chr	Pos	Ref	Alt	Mock		AAVS1		Type	Feature	Gene	Change	Homology to gRNA?
				VAF	Cov	VAF	Cov					
chr1	22511138	T	G	0.004	948	0.078	994	SNV	intron	*ZBTB40*		No
chr1	163339479	T	G	0.000	851	0.031	795	SNV	intron	*NUF2*		No
chr1	231162978	A	C	0.003	1172	0.118	1131	SNV	exon	*TRIM67*	missense (E3D)	No
chr3	75665744	G	A	0.010	983	0.017	919	SNV	exon	*FRG2C*	silent	No
chr3	113657339	T	G	0.001	1049	0.057	1052	SNV	exon	*USF3*	missense (Q1448P)	No
chr3	171084160	A	C	0.009	643	0.111	709	SNV	exon	*TNIK*	missense (L1055R)	No
chr4	150849453	A	C	0.000	1001	0.012	1021	SNV	exon	*LRBA*	missense (L1376R)	No
chr4	150849456	A	C	0.001	1035	0.016	1044	SNV	exon	*LRBA*	missense (I1375R)	No
chr5	3610294	A	C	0.001	1353	0.073	1351	SNV	intergenic			No
chr6	31027750	T	G	0.001	1105	0.079	1040	SNV	exon	*MUC22*	silent	No
chr6	89265707	CAAG	C	0.007	1016	0.020	1146	3bp del	exon	*GABRR2*	in-frame	No
chr7	74219789	T	G	0.000	1320	0.077	1206	SNV	intron	*LAT2*		No
chr7	75999137	CAAAA	C	0.000	240	0.025	239	3bp del	intron	*STYXL1*		No
chr7	78135069	T	G	0.000	1180	0.130	1090	SNV	exon	*MAGI2*	missense (I995L)	No
chr7	137466949	GA	G	0.009	885	0.028	1004	1bp del	intron	*DGK1*		No
chr8	70141198	T	G	0.000	959	0.043	961	SNV	exon	*NCOA2*	missense (Q1005P)	No
chr8	124067789	GA	G	0.006	1072	0.016	1076	1bp del	exon	*FER1L6*	frameshift	No
chr9	124869379	C	A	0.003	905	0.013	857	SNV	exon	*ARPC5L*	missense (A30E)	No
chr10	102157285	CGAG	C	0.010	1023	0.023	967	3bp del	exon	*NOLC1*	in-frame	No
chr12	52287653	A	C	0.006	941	0.043	868	SNV	exon	*KRT81*	missense (N323K)	No
chr16	29806124	ACCTC	A	0.010	401	0.023	428	4bp del	5' UTR	*MAZ*		No
chr16	57452819	CGAG	C	0.009	1416	0.017	1371	3bp del	exon	*COQ9*	in-frame	No
chr17	28644104	C	CA	0.005	1207	0.015	1171	1bp ins	exon	*KIAA0100*	frameshift	No
chr17	38810572	CT	C	0.007	1215	0.017	1236	1bp del	exon	*CWC25*	frameshift	No
chr18	79396207	CCCG	C	0.004	836	0.018	718	3bp del	5' UTR	*NFATC1*		No
chr19	10805866	TC	T	0.003	1270	0.017	1192	1bp del	intron	*DNM2*		No
chr19	11447576	G	A	0.003	882	0.010	981	SNV	exon	*PRKCSH*	silent	No
chr19	35618460	A	C	0.003	1099	0.062	1038	SNV	exon	*HAUS5*	missense (I294L)	No
chr21	46432047	GGA	G	0.010	1074	0.023	986	2bp del	exon	*PCNT*	frameshift	No
chrX	85964085	TTA	T	0.010	815	0.020	850	2bp del	intron	*CHM*		No

a) VAF x Coverage for all variants called by exome sequencing pipeline in Mock and AAVS1 d10 conditions. Large white points are those that remained after removing germline and synonymous variants. Large black points are those that remain after removing variants present in Mock within each donor.

b) VAF for variants called by tumor-normal pipeline when AAVS1 is used as tumor and Mock as normal inputs (left panel), and when Mock is used as tumor and AAVS1 as normal (right panel).

c) VAF x Coverage for 137 variants shown in Panel B. 30 large white points are those that remained after removing variants with Mock VAF >0.01.

d) Annotation for all 30 AAVS1 variants. Homology to gRNA is defined as 10 or more matches to protospacer+PAM within 20bp upstream or downstream of variant.

Supplemental Table 1: Genes included on TSO500 panel.

ABL1	BRD4	CUX1	FAM175A	GATA6	IGF1	MAP3K13	NOTCH4	POLE	RPTOR	TAF1
ABL2	BRIP1	CXCR4	FAM46C	GEN1	IGF1R	MAP3K14	NPM1	PPARG	RUNX1	TBX3
ACVR1	BTG1	CYLD	FANCA	GID4	IGF2	MAP3K4	NRAS	PPM1D	RUNX1T1	TCEB1
ACVR1B	BTK	DAXX	FANCC	GLI1	IKBKE	MAPK1	NRG1	PPP2R1A	RYBP	TCF3
AKT1	C11orf30	DCUN1D1	FANCD2	GNA11	IKZF1	MAPK3	NSD1	PPP2R2A	SDHA	TCF7L2
AKT2	CALR	DDR2	FANCE	GNA13	IL10	MAX	NTRK1	PPP6C	SDHAF2	TERC
AKT3	CARD11	DDX41	FANCF	GNAQ	IL7R	MCL1	NTRK2	PRDM1	SDHB	TERT
ALK	CASP8	DHX15	FANCG	GNAS	INHA	MDC1	NTRK3	PREX2	SDHC	TET1
ALOX12B	CBFB	DICER1	FANCI	GPR124	INHBA	MDM2	NUP93	PRKAR1A	SDHD	TET2
ANKRD11	CBL	DIS3	FANCL	GPS2	INPP4A	MDM4	NUTM1	PRKCI	SETBP1	TFE3
ANKRD26	CCND1	DNAJB1	FAS	GREM1	INPP4B	MED12	PAK1	PRKDC	SETD2	TFRC
APC	CCND2	DNMT1	FAT1	GRIN2A	INSR	MEF2B	PAK3	PRSS8	SF3B1	TGFBR1
AR	CCND3	DNMT3A	FBXW7	GRM3	IRF2	MEN1	PAK7	PTCH1	SH2B3	TGFBR2
ARAF	CCNE1	DNMT3B	FGF1	GSK3B	IRF4	MET	PALB2	PTEN	SH2D1A	TMEM127
ARFRP1	CD274	DOT1L	FGF10	H3F3A	IRS1	MGA	PARK2	PTPN11	SHQ1	TMPRSS2
ARID1A	CD276	E2F3	FGF14	H3F3B	IRS2	MITF	PARP1	PTPRD	SLIT2	TNFAIP3
ARID1B	CD74	EED	FGF19	H3F3C	JAK1	MLH1	PAX3	PTPRS	SLX4	TNFRSF14
ARID2	CD79A	EGFL7	FGF2	HGF	JAK2	MLL	PAX5	PTPRT	SMAD2	TOP1
ARID5B	CD79B	EGFR	FGF23	HIST1H1C	JAK3	MLLT3	PAX7	QKI	SMAD3	TOP2A
ASXL1	CDC73	EIF1AX	FGF3	HIST1H2BD	JUN	MPL	PAX8	RAB35	SMAD4	TP53
ASXL2	CDH1	EIF4A2	FGF4	HIST1H3A	KAT6A	MRE11A	PBRM1	RAC1	SMARCA4	TP63
ATM	CDK12	EIF4E	FGF5	HIST1H3B	KDM5A	MSH2	PDCD1	RAD21	SMARCB1	TRAF2
ATR	CDK4	EML4	FGF6	HIST1H3C	KDM5C	MSH3	PDCD1LG2	RAD50	SMARCD1	TRAF7
ATRX	CDK6	EP300	FGF7	HIST1H3D	KDM6A	MSH6	PDGFRA	RAD51	SMC1A	TSC1
AURKA	CDK8	EPCAM	FGF8	HIST1H3E	KDR	MST1	PDGFRB	RAD51B	SMC3	TSC2
AURKB	CDKN1A	EPHA3	FGF9	HIST1H3F	KEAP1	MST1R	PDK1	RAD51C	SMO	TSHR
AXIN1	CDKN1B	EPHA5	FGFR1	HIST1H3G	KEL	MTOR	PDPK1	RAD51D	SNCAIP	U2AF1
AXIN2	CDKN2A	EPHA7	FGFR2	HIST1H3H	KIF5B	MUTYH	PGR	RAD52	SOCS1	VEGFA
AXL	CDKN2B	EPHB1	FGFR3	HIST1H3I	KIT	MYB	PHF6	RAD54L	SOX10	VHL
B2M	CDKN2C	ERBB2	FGFR4	HIST1H3J	KLF4	MYC	PHOX2B	RAF1	SOX17	VTCN1
BAP1	CEBPA	ERBB3	FH	HIST2H3A	KLHL6	MYCL1	PIK3C2B	RANBP2	SOX2	WISP3
BARD1	CENPA	ERBB4	FLCN	HIST2H3C	KMT2B	MYCN	PIK3C2G	RARA	SOX9	WT1
BBC3	CHD2	ERCC1	FLI1	HIST2H3D	KMT2C	MYD88	PIK3C3	RASA1	SPEN	XIAP
BCL10	CHD4	ERCC2	FLT1	HIST3H3	KMT2D	MYOD1	PIK3CA	RB1	SPOP	XPO1
BCL2	CHEK1	ERCC3	FLT3	HLA-A	KRAS	NAB2	PIK3CB	RBM10	SPTA1	XRCC2
BCL2L1	CHEK2	ERCC4	FLT4	HLA-B	LAMP1	NBN	PIK3CD	RECQL4	SRC	YAP1
BCL2L11	CIC	ERCC5	FOXA1	HLA-C	LATS1	NCOA3	PIK3CG	REL	SRSF2	YES1
BCL2L2	CREBBP	ERG	FOXL2	HNF1A	LATS2	NCOR1	PIK3R1	RET	STAG1	ZBTB2
BCL6	CRKL	ERRFI1	FOXO1	HNRNPK	LMO1	NEGR1	PIK3R2	RFWD2	STAG2	ZBTB7A
BCOR	CRLF2	ESR1	FOXP1	HOXB13	LRP1B	NF1	PIK3R3	RHEB	STAT3	ZFHX3
BCORL1	CSF1R	ETS1	FRS2	HRAS	LYN	NF2	PIM1	RHOA	STAT4	ZNF217
BCR	CSF3R	ETV1	FUBP1	HSD3B1	LZTR1	NFE2L2	PLCG2	RICTOR	STAT5A	ZNF703
BIRC3	CSNK1A1	ETV4	FYN	HSP90AA1	MAGI2	NFKBIA	PLK2	RIT1	STAT5B	ZRSR2
BLM	CTCF	ETV5	GABRA6	ICOSLG	MALT1	NKX2-1	PMAIP1	RNF43	STK11	
BMPR1A	CTLA4	ETV6	GATA1	ID3	MAP2K1	NKX3-1	PMS1	ROS1	STK40	
BRAF	CTNNA1	EWSR1	GATA2	IDH1	MAP2K2	NOTCH1	PMS2	RPS6KA4	SUFU	
BRCA1	CTNNB1	EZH2	GATA3	IDH2	MAP2K4	NOTCH2	PNRC1	RPS6KB1	SUZ12	
BRCA2	CUL3	FAM123B	GATA4	IFNGR1	MAP3K1	NOTCH3	POLD1	RPS6KB2	SYK	

Content shaded in grey is analyzed for CNV detction.

Supplemental Table 2: Cas9 gRNA information.

Target	**Guide Sequence**	**Location (hg19)**	**Location (hg38)**	**Strand**
AAVS1	GGGGCCACTAGGGACAGGAT(NGG)	chr19:55627117-55627139	chr19:55115752-55115771	-
HBB	CTTGCCCCACAGGGCAGTAA(NGG)	chr11:5248198-5248220	chr11:5226968-5226987	+
ZFPM2	AATGATGACGATGATGATGA(NGG)	chr8:106499982-106500004	chr8:105487754-105487776	-

Supplemental Figure 1: Bioinformatic pipeline used to align reads with genome

a

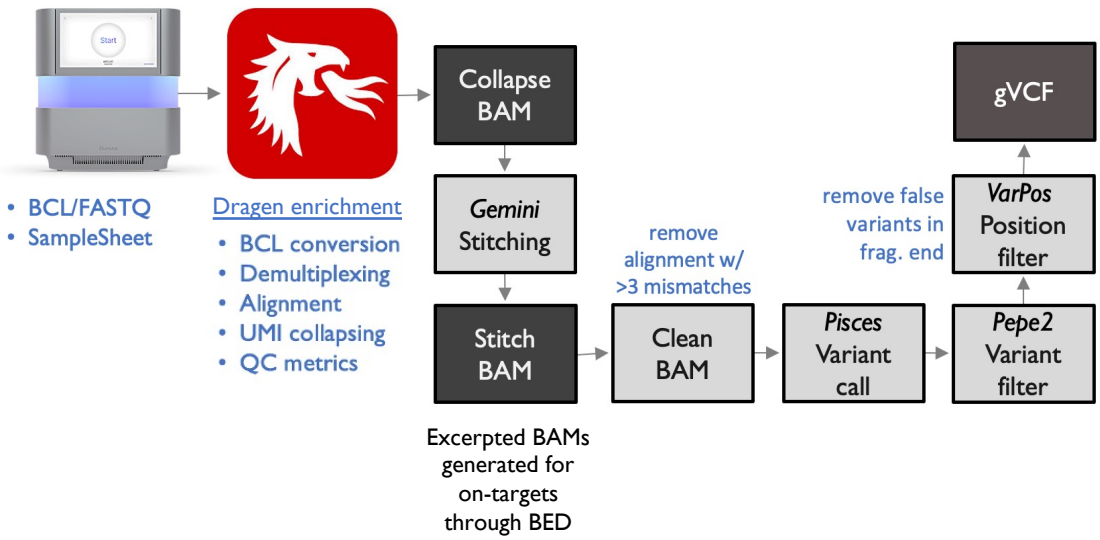

b

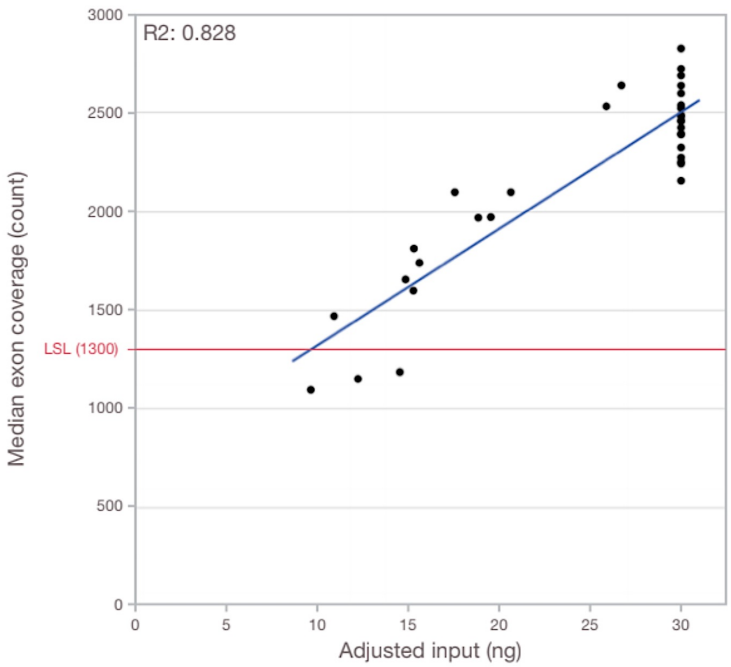

a) Bioinformatics pipeline used to map reads to genome, call, and annotate variants.
b) DNA input and corresponding MEC yielded in pilot library prep and sequencing runs. LSL = recommended lower specification limit, set at 1300 MEC.

Supplemental Table 3: Supplementary probe information

Chromosome	Start	Stop	Name
chr19	55626110	55626230	AAVS1
chr19	55626230	55626350	AAVS1
chr19	55626350	55626470	AAVS1
chr19	55626470	55626590	AAVS1
chr19	55626590	55626710	AAVS1
chr19	55626710	55626830	AAVS1
chr19	55626830	55626950	AAVS1
chr19	55626950	55627070	AAVS1
chr19	55627070	55627190	AAVS1
chr19	55627190	55627310	AAVS1
chr19	55627310	55627430	AAVS1
chr19	55627430	55627550	AAVS1
chr19	55627550	55627670	AAVS1
chr19	55627670	55627790	AAVS1
chr19	55627790	55627910	AAVS1
chr19	55627910	55628030	AAVS1
chr19	55628030	55628150	AAVS1
chr11	5246772	5246892	*HBB*
chr11	5246892	5247012	*HBB*
chr11	5247797	5247917	*HBB*
chr11	5247917	5248037	*HBB*
chr11	5248145	5248265	*HBB*
chr8	106331145	106331265	*ZFPM2*
chr8	106431331	106431451	*ZFPM2*
chr8	106431451	106431571	*ZFPM2*
chr8	106456498	106456618	*ZFPM2*
chr8	106573590	106573710	*ZFPM2*
chr8	106646469	106646589	*ZFPM2*
chr8	106800929	106801049	*ZFPM2*
chr8	106801049	106801169	*ZFPM2*
chr8	106810943	106811063	*ZFPM2*
chr8	106811063	106811183	*ZFPM2*
chr8	106813260	106813380	*ZFPM2*
chr8	106813380	106813500	*ZFPM2*
chr8	106813500	106813620	*ZFPM2*
chr8	106813620	106813740	*ZFPM2*
chr8	106813740	106813860	*ZFPM2*
chr8	106813860	106813980	*ZFPM2*
chr8	106813980	106814100	*ZFPM2*
chr8	106814100	106814220	*ZFPM2*
chr8	106814220	106814340	*ZFPM2*
chr8	106814340	106814460	*ZFPM2*
chr8	106814460	106814580	*ZFPM2*
chr8	106814580	106814700	*ZFPM2*
chr8	106814700	106814820	*ZFPM2*
chr8	106814820	106814940	*ZFPM2*
chr8	106814940	106815060	*ZFPM2*
chr8	106815060	106815180	*ZFPM2*
chr8	106815180	106815300	*ZFPM2*
chr8	106815300	106815420	*ZFPM2*
chr8	106815420	106815540	*ZFPM2*
chr8	106815540	106815660	*ZFPM2*
chr8	106815660	106815780	*ZFPM2*

36 probes were designed for the two gene symbol inputs by IDT (*HBB* and *ZFPM2*). Bed coordinates are shown in hg19 assemblies. For gene capture panels (i.e., *HBB* and *ZFPM2*), the probes come from IDT's xGen Exome Research Panel. They are spaced at 1x tiling where every base is covered by at least one probe. The original exome design was performed with repeat masking and empirically validated so we do not perform any additional QC to the probe sequences.

For AAVS1, we padded probes 1kb upstream and downstream (120bp probes collectively hybridized to all exons with at least 1x tiling, meaning each base is covered by at least one probe). For SNPs, we padded out to 100bp with all SNPs directly in the middle. We then designed at 1x tiling without repeat masking and IDT performed predictive QC analysis to the probe sequences. The QC analysis involved standard BLAST and Minimap alignment.

Supplemental Figure 2: Calculation of limit of detection & sensitivity given MEC

a

Limit of Detection (VAF)	Sensitivity	Minimum MEC
0.1%	95%	7752
0.1%	90%	6679
0.2%	95%	3875
0.2%	90%	3339
0.5%	95%	1258
0.5%	90%	1063

b

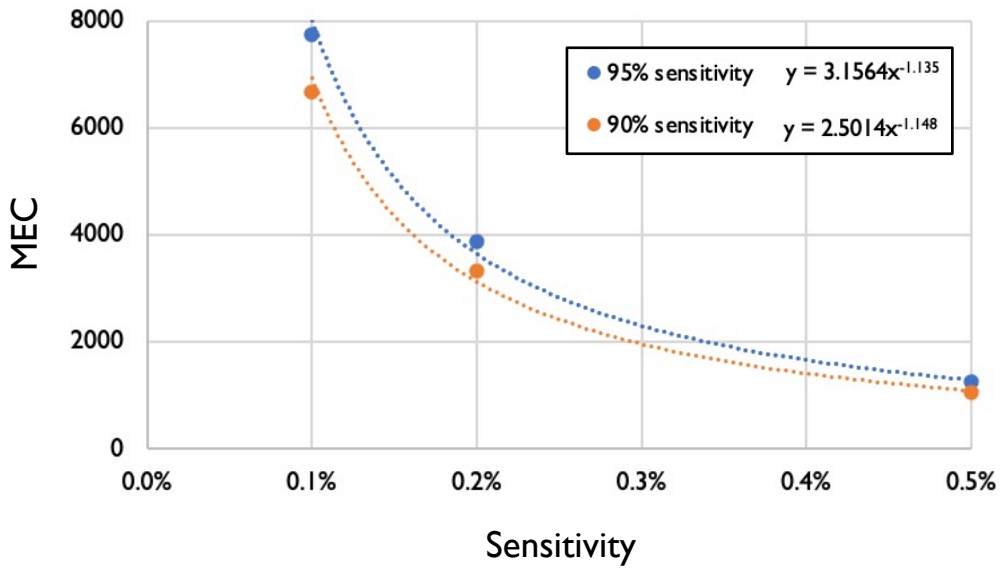

Plot of MEC by sensitivity according to table in Panel A. Dotted line depicts the power trendline and equation of the line is shown in the figure legend.

c

We first define a likely score "L" to quantify sensitivity of variant detection.

$L = \log_{10}(\text{dbinom}(x,MEC,AF)/ \text{dbinom}(x,MEC,er))$
Where "er" = 1e-5 (i.e., 99.999% specificity), "AF" = allele frequency = x/MEC, and "dbinom" is the density of a binomial function b(x, n, p), "x" is the number of times for a specific outcome within n trials, each with probability of success, p, on a single trial;

Next, we define a threshold "t" as the minimal number of x that satisfies $L \geq 2$ (i.e., the true signal needs to be 100 times or more than error.)

Hence, the sensitivity and "LoD" is given by:
Sensitivity = 1-pbinom(t-1,MEC,LoD),
Where "pbinom" is the cumulative probability of (t-1) or less successful trails from MEC binomial trials, each with LoD probability of success.

Supplemental Table 4: Reproducibility across technical replicates.

Donor	Treatment	Day	# technical replicates	% sites present in all technical replicates (reproducible/total)
1	-	0	2	98.88% (1496/1513)
1	Mock	4	3	98.36% (1497/1522)
1	Mock	10	3	96.39% (1494/1550)
1	AAVS1	4	3	96.89% (1496/1544)
1	AAVS1	10	3	97.39% (1491/1531)
1	*HBB*	4	3	97.52% (1493/1531)
1	*HBB*	10	3	97.77% (1492/1526)
1	*ZFPM2*	4	3	90.75% (1491/1643)
1	*ZFPM2*	10	3	97.39% (1493/1533)
2	-	0	3	99.05% (1462/1476)
2	Mock	4	1	100.00% (1475/1475)
2	Mock	10	2	99.19% (1473/1485)
2	AAVS1	4	3	98.71% (1453/1472)
2	AAVS1	10	3	98.12% (1461/1489)
2	*HBB*	4	3	98.38% (1454/1478)
2	*HBB*	10	3	97.66% (1458/1493)
2	*ZFPM2*	4	1	100.00% (1474/1474)
2	*ZFPM2*	10	3	98.60% (1476/1497)
3	-	0	3	98.88% (1504/1521)
3	Mock	4	3	98.43% (1504/1528)
3	Mock	10	3	97.54% (1506/1544)
3	AAVS1	4	3	97.22% (1501/1544)
3	AAVS1	10	3	97.09% (1501/1546)
3	*HBB*	4	3	98.43% (1504/1528)
3	*HBB*	10	3	97.79% (1503/1537)
3	*ZFPM2*	4	2	98.13% (1522/1551)
3	*ZFPM2*	10	2	99.15% (1519/1532)

Supplemental Figure 3: Read depth across variants

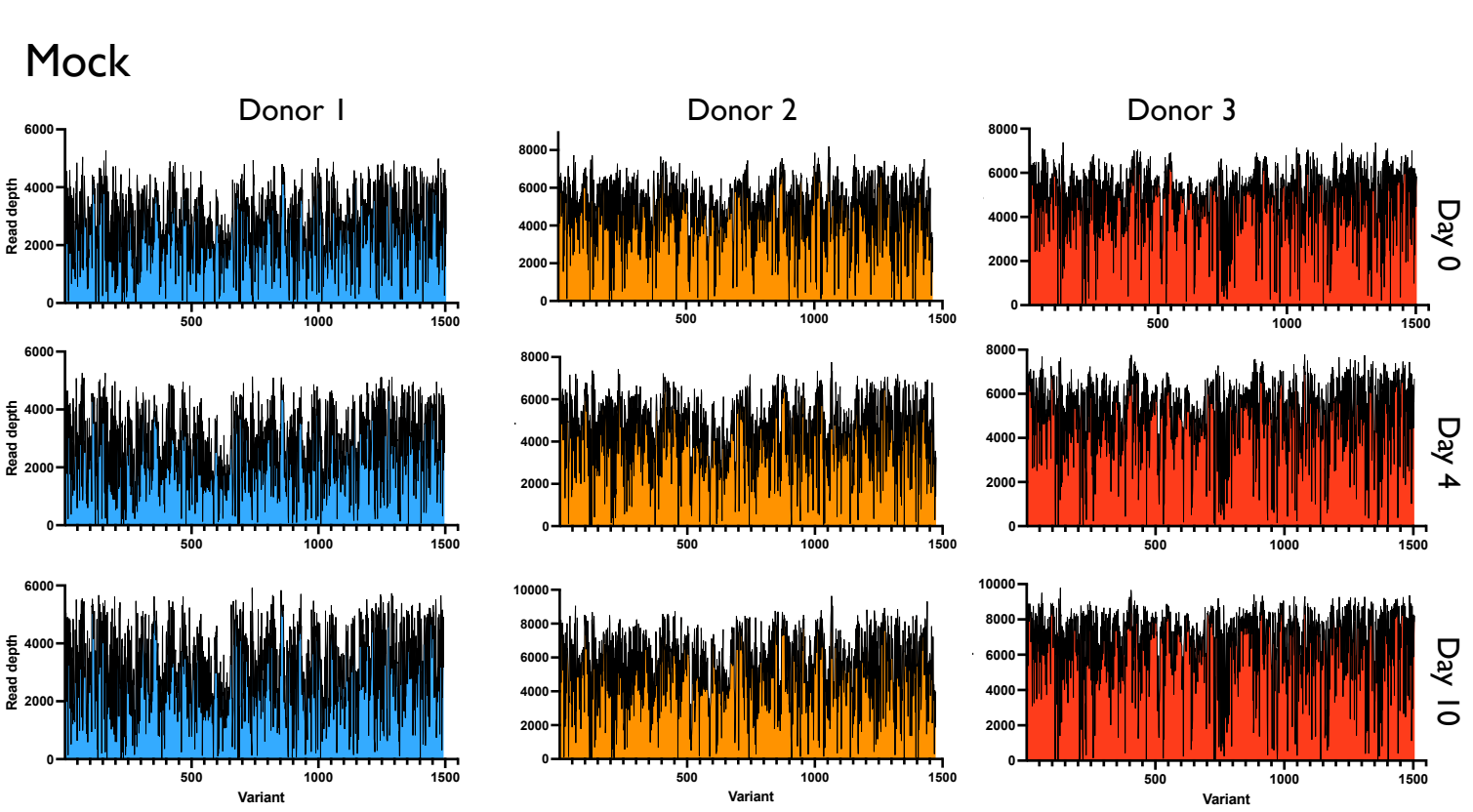

Supplemental Figure 4: Read depth across variants

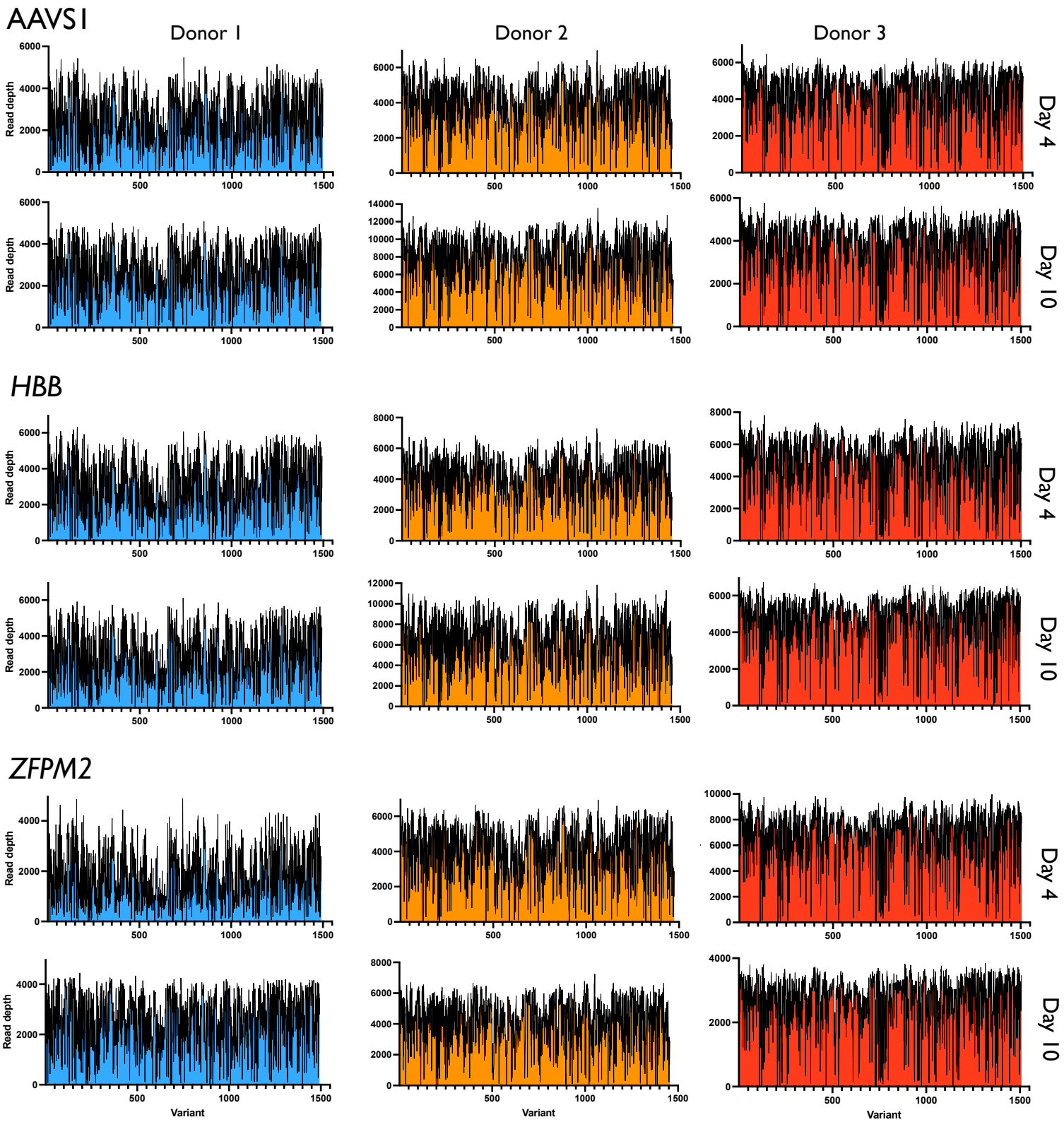

Depicted is read depth across all reproducible variants within each treatment and donor. All variants were ordered numerically across genomic coordinates, beginning with chromosome 1 on the left end of the x-axis and ending with the sex chromosomes on the right end of the axis.

Supplemental Figure 4:Variants found in treatment groups.

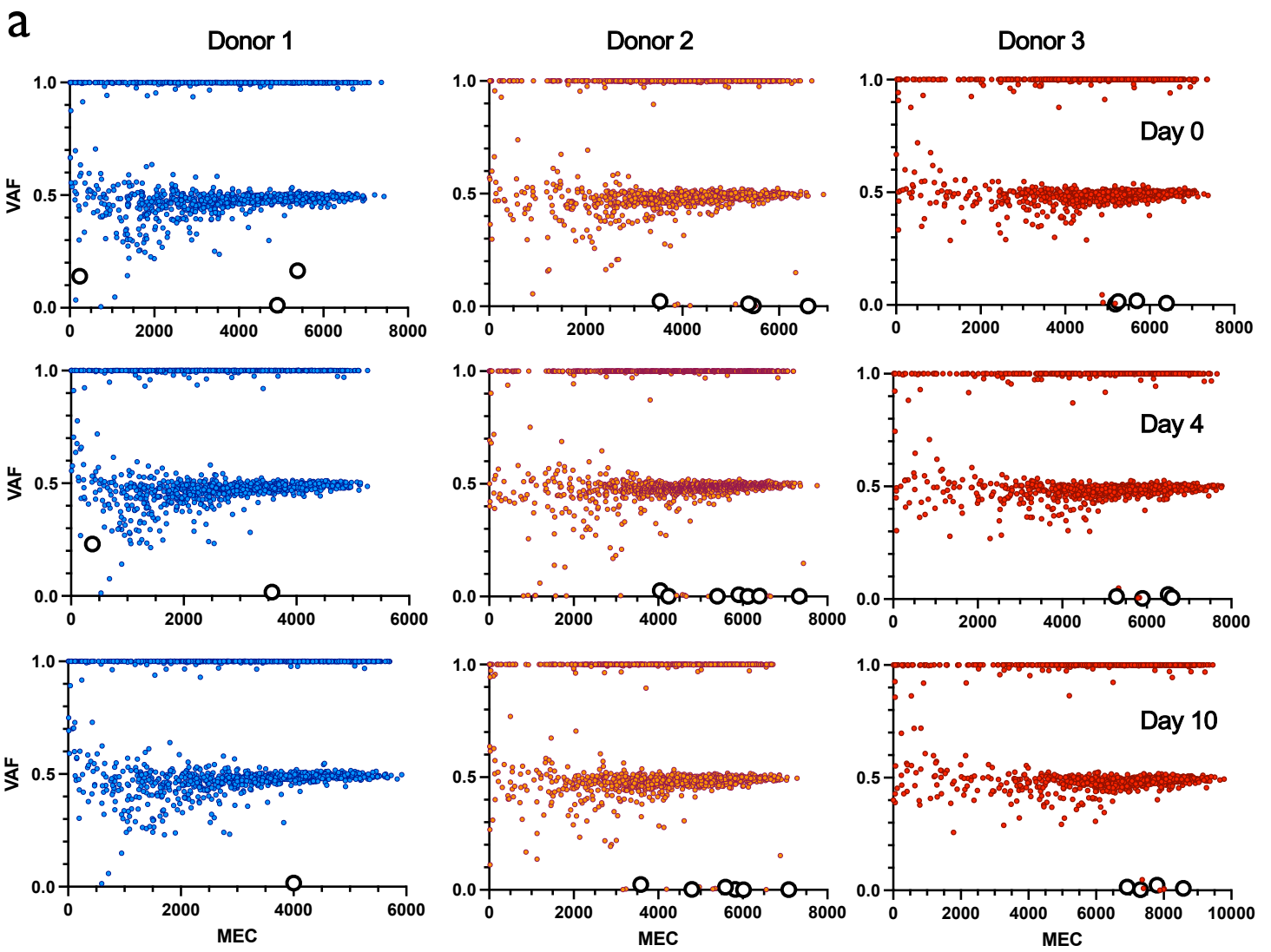

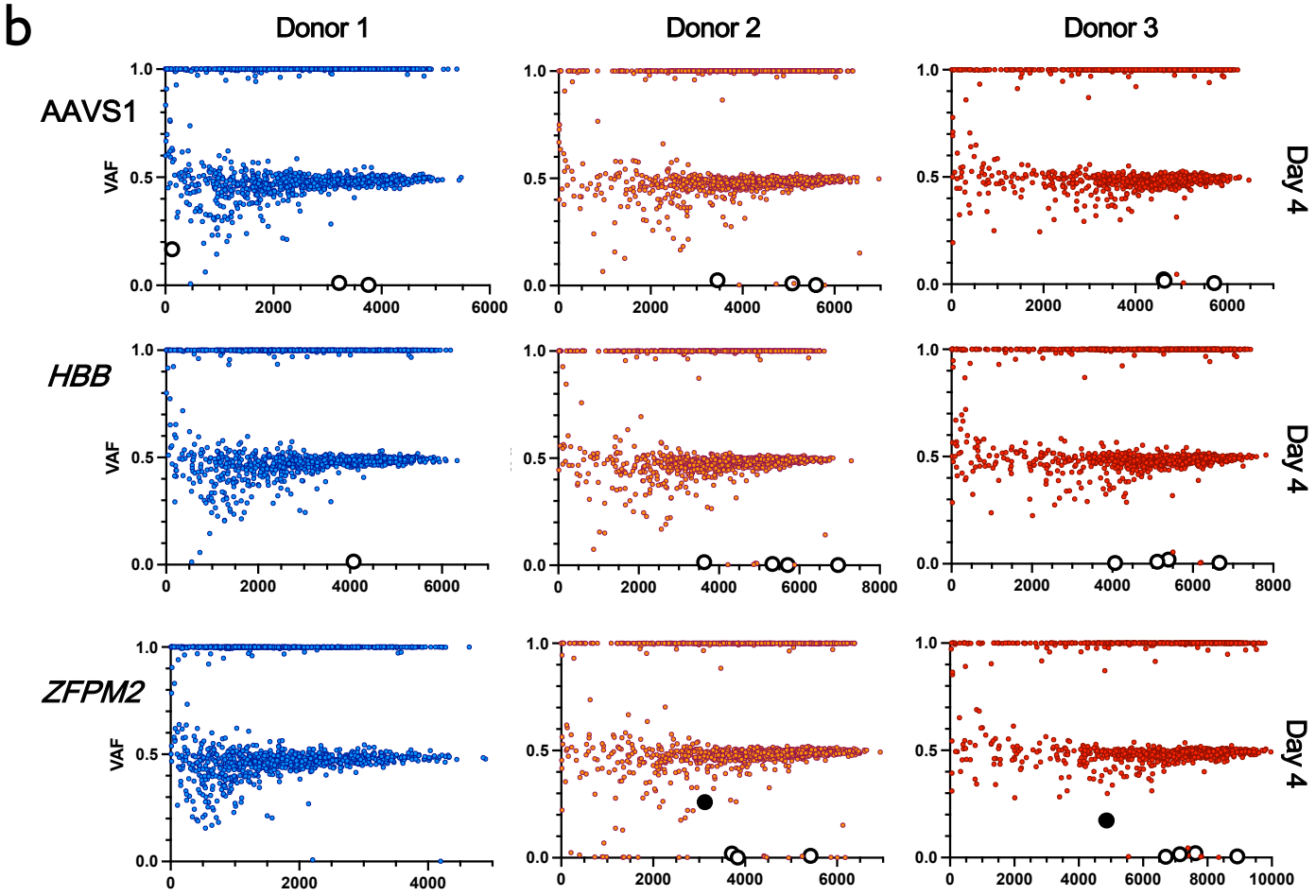

a) VAF x MEC for all variants found among technical replicates for Mock treatment for each donor at d0, d4, and d10. Large white points are those that remained after removing germline and synonymous variants.

b) VAF x MEC for all variants found among technical replicates for Cas9 treatments for each donor at d4. Large white points are those that remained after removing germline and synonymous variants. Large black points are those that remain after removing variants present in Mock within each donor.

Supplemental Figure 5: Indel size distribution & frequency for *EZH2*

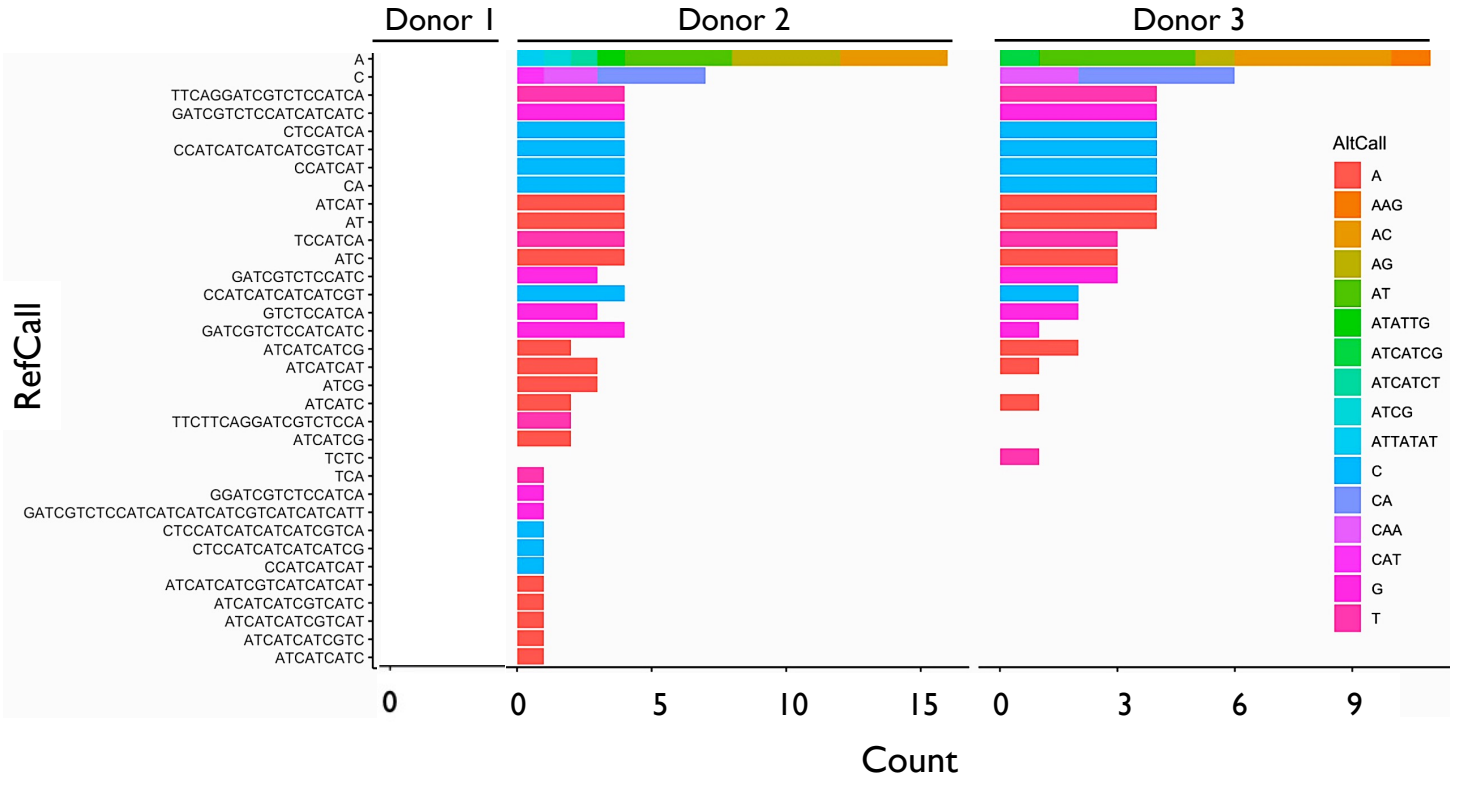

Specific indels within *EZH2* for each donor in *ZFPM2* treatments (d4 and 10 are combined). Y-axis depicts the normal genome reference call ("RefCall") and rows depict the frequency at which alternative variant calls ("AltCall") are found within *EZH2*. Note: no *EZH2* indels detected in Donor 1.

Supplemental Figure 6: Genes harboring indels among donors, timepoints, & Cas9 treatments

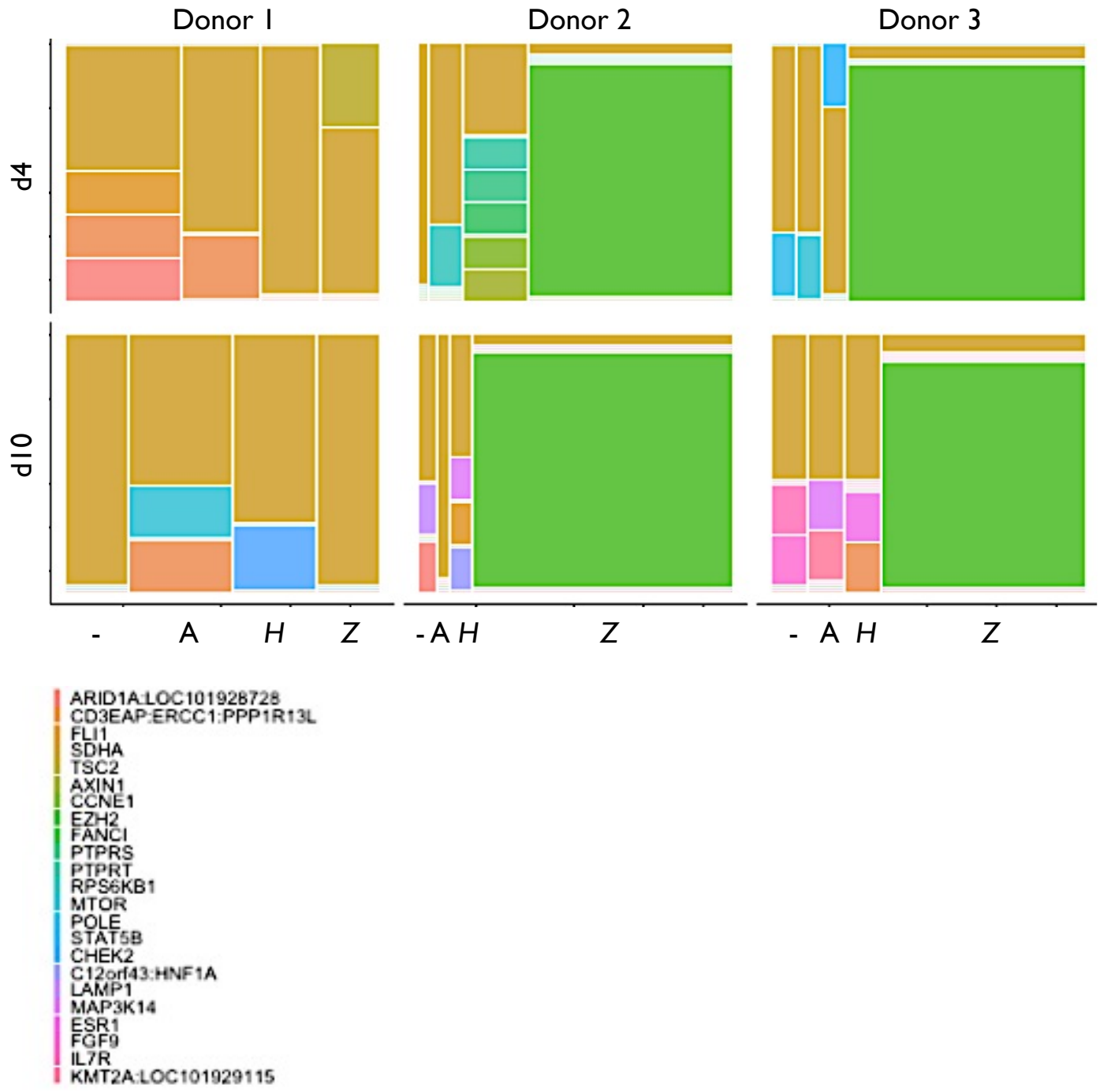

Mosaic plot of genes harboring indels within each donor and Cas9 treatment at d4 and 10 (Mock = -, AAVS1 = A, *HBB* = *H*, and *ZFPM2* = *Z*). Area is proportional to the number of times variants were called within a particular gene within a particular treatment group. Filtering removed germline and synonymous variants as well as MNVs and SNVs.